XVII[èmes] *Journées Nationales Génie Côtier – Génie Civil*
Chatou, 2022
DOI:10.5150/jngcgc.2022.002 *© Editions Paralia CFL*
disponible en ligne – http://www.paralia.fr – available online

Open-FOAM computations of breaking wave impact on a vertical wall with a recurved parapet

Yasmine BEN BELKACEM [1,2], Gaële PERRET [1], Julie LEBUNTEL [2], Grégory PINON [1]

1. Laboratoire Ondes et Milieux Complexes, UMR 6294 CNRS, Université Le Havre Normandie, 76600 Le Havre, France.
   yasmine.ben-belkacem@univ-lehavre.fr; gaele.perret@univ-lehavre.fr ; gregory.pinon@univ-lehavre.fr
2. INGEROP Conseil et Ingénierie, Agence de Rennes, 12 rue du Pâtis Tatelin, CS 50891, 35708 Rennes, France.
   julie.lebunetel@ingerop.com

Abstract:
The present paper describes the numerical approach used for the computations of breaking wave impact on a vertical wall with a recurved parapet. The simulations will concern the configuration at 1:1 large scale (RAVINDAR *et al*., 2019, 2020; RAVINDAR & SRIRAM, 2021), for which experiments were performed in Coastal Research Centre (Forschungs Zentrum Küste, FZK), Hannover, Germany.
In terms of numerical code, the *OpenFOAM* numerical toolbox will be used. In the considered *InterFOAM* solver, the Navier–Stokes equations are solved for the simulation of a two-phase flow, combined with a Volume of Fluid (VOF) for tracking the free surface and the PIMPLE algorithm for resolving the pressure-velocity equations. Moreover, the relaxation zone module of the *waves2Foam toolbox* as introduced by JACOBSEN *et al*., (2012) is presently used for waves generation and propagation. Also, in order to better assess possible impulsive impacts, either a compressible or incompressible version of the code will be used following the methodology presented in BATLLE MARTIN *et al*., (2021).

Keywords:
Breaking wave, Impact pressure, Open-FOAM, Wave generation, Compressibility effects.

1. Introduction

Offshore and coastal structures such as sea walls, which are located in intermediate water depth or in shallow water, are being damaged when subjected to extreme sea state conditions. Therefore, the investigation of wave-structure interactions is a key factor in the safe and cost-effective design of the coastal structures.

Experiments are one of the most common approaches used for studying the wave loading. The first documentation of this latter dates from 1937 when DE ROUVILLE *et al*., (1938) used wave gauges and piezo-electric transducers in the port of Dieppe (France) to record a large-scale impact pressure. Afterwards, several laboratory experiments (smaller scale) were conducted to characterize and measure the impact pressures due to the collisions of non-breaking and breaking waves against a vertical structure/wall (OUMERACI *et al*., 1993).

The extreme impact pressure problem has been also underlined theoretically by COOKER & PEREGRINE (1990) who proposed an analytical model based on the impulse theory. Moreover, with the significant advances of High-Performance Computation, several numerical simulations were carried out to provide accurate predictions for wave loading, using different Computational Fluid Dynamics (CFD) tools. But more recently, the open-source library OpenFOAM based on the Finite Volume Method (FVM) and using the Volume of Fluid (VoF) approach has been applied to investigate various problems related to coastal and offshore engineering. The good capabilities of this software were demonstrated by MORGAN *et al*., (2010) and LIU *et al*., (2019).

In the present work, the multiphase incompressible and compressible solvers from the OpenFOAM package combined with the waves2FOAM toolbox (JACOBSEN *et al*., 2012), are used to simulate the waves propagating and impacting on a vertical wall. More precisely, the aim of this study, is to reproduce numerically the free surface behaviour and the pressure impact of a breaking wave on a vertical wall within a large-scale configuration for which experiments were performed by RAVINDAR *et al*., (2019) and RAVINDAR & SRIRAM (2021).

Different wave gauges present in the experimental configuration, will be used as input parameters for our computations. Additional pressure probes and wave gauges will be used for the validation of our numerical approach by numerical-experimental cross-comparison.

2. Numerical Model

2.1 Governing equations

The *interFoam* or *compressible* solver within the OpenFOAM framework is used to carry out this study. It solves the 3D unsteady Navier-Stokes equations for a homogenous and immiscible two-phase fluid.

The Navier-Stokes governing equations are written as a mass conservation equation (equation 1) and a single momentum balance equation (equation 2) modelling both phases, such as:

$$\frac{\partial \rho}{\partial t} + \nabla.(\partial \boldsymbol{u}) = 0, \quad (1)$$

$$\frac{\partial \rho \boldsymbol{u}}{\partial t} + \nabla.(\rho \boldsymbol{u}\boldsymbol{u}) = -\nabla p + \nabla.\left[\mu\left(\nabla \boldsymbol{u} + (\nabla \boldsymbol{u})^T - \frac{2}{3}(\nabla.\boldsymbol{u})\underline{\boldsymbol{I}}\right)\right] + \boldsymbol{S}, \quad (2)$$

where ρ is the fluid density, $\boldsymbol{u}$ the velocity vector, p is the pressure, μ is the dynamic viscosity and $\boldsymbol{S}$ stands for the body force term.
When the fluid is assumed to be incompressible, equation (1) turns into:

$$\nabla.\boldsymbol{u} = 0, \quad (3)$$

and equation (2) takes the general form presented as follows:

$$\rho\left(\frac{\partial \boldsymbol{u}}{\partial t} + \boldsymbol{u}.\nabla \boldsymbol{u}\right) = -\nabla p + \mu \nabla^2 \boldsymbol{u} + \boldsymbol{S}. \quad (4)$$

The spatial discretization of these equations is performed by the Finite Volume Method (FVM) based on an unstructured mesh with arbitrary continuous polyhedral cells. In addition, the PIMPLE algorithm, which is a merge of the PISO (Pressure Implicit with Splitting of Operator) (ISSA, 1986) and SIMPLE (Semi-Implicit Method for Pressure-Linked Equations) (FERZIGER & PERIC, 1999), is used to fully solve the pressure-velocity coupling for each time step. The velocity field and pressure are afterwards corrected several times to satisfy the continuity equation. The linear solver called Geometric-Algebraic Multi-Grid (GAMG) is used to solve the set of these linear equations.
Additionally, time-derivatives are discretized by the implicit Euler scheme and the Gaussian interpolation is applied to the gradient operators.
In order to increase the stability and the accuracy of our numerical model, a self-adjusting time step Δt is applied. This latter is adapted at the beginning of every new time loop according to the given maximum Courant Number *Co* (COURANT *et al.*, 1967). The Courant Number is defined as follows:

$$Co = \frac{\Delta t}{\Delta x}|U|, \quad (5)$$

where Δt is the maximum time step, Δx is the cell size and $|U|$ is the velocity magnitude. The maximum Courant number value should be below 1 throughout the whole domain.

2.2 Free surface treatment

The Volume of Fluid (VoF) technique, presented by HIRT and NICHOLS (1981), is employed for free surface tracking. In fact, the two-phase domain is considered as a Eulerian mixture and each of the two phases ($\mathcal{A}$ for water and $\mathcal{B}$ for air) has a separately

defined volume fraction denoted by $\alpha_{\mathcal{A}}$ and $\alpha_{\mathcal{E}}$ respectively such as $\alpha_{\mathcal{A}} + \alpha_{\mathcal{E}} = 1$ in each computational cell. The volume fraction function is defined as:

$$\alpha = \begin{cases} 0, & air \\ 0 < \alpha < 1, & air - water\ interface \\ 1, & water \end{cases} \quad (6)$$

The volume fraction is advected by the following transport equation:

$$\frac{\partial \alpha}{\partial t} + \nabla . (\alpha\, \boldsymbol{u}) = 0. \quad (7)$$

The advection equation (8) is slightly modified by an algebraic method, as follows:

$$\frac{\partial \alpha}{\partial t} + \nabla . (\alpha\, \boldsymbol{u}) + \nabla . (\boldsymbol{u_r}\, \alpha\, (1 - \alpha)) = 0, \quad (8)$$

where the extra term on the left-hand side of equation (8) represents an artificial compression, which ensures the non-smearing of the free surface and limit the numerical diffusion, and $\boldsymbol{u_r}$ is the relative compression velocity. In the solving procedure, the Multidimensional Universal Limiter with Explicit Solution (MULES) is used for this purpose.

2.3 Waves modelling

The *waves2Foam* toolbox is used for generating different incident wave theories and absorbing the reflected ones. In this numerical approach, the compressible /incompressible solver is coupled with the relaxation zones (RZ) method (JACOBSEN *et al.*, 2012). The RZs are added in the numerical wave tank to gradually blend between a target φ_{target} and a computed $\varphi_{computed}$ solution and force them to match at the boundary. This blending procedure is applied each time step on the velocity and VoF fields. The blending function is defined in the following way:

$$\varphi(x,t) = \alpha_R(x)\varphi_{computed}(x,t) + (1 - \alpha_R(x)\varphi_{target}(x,t), \quad (9)$$

where α_R is a weight field (FUHRMAN *et al.*, 2006), and reads:

$$\alpha_R = 1 - \frac{e^{\chi^{3.5}} - 1}{e^1 - 1}. \quad (10)$$

3. Numerical results and discussion

3.1 Grid mesh convergence study for the wave's propagation

In order to assess the capabilities of the relaxation zone method for generating and absorbing Stokes second order waves, a validation study was carried out. This study focuses on a simple rectangular numerical wave tank (NWT) in 2D. The total length of the computational domain is 243m which represents about 5 wave lengths (λ) in the wave

propagation direction. The inlet and outlet relaxation zones have a length of λ and 3λ respectively, allowing a proper generation and absorption of the incident wave.
A monochromatic Stokes second order waves with a wave height of H = 0.5m and a period of T = 6s were generated at a water depth of h = 8m. As far as the boundary conditions are concerned, atmospheric conditions, with a total pressure and zero-gradient velocity, were assigned to the top boundary. The bottom boundary is defined as a solid wall with a no-slip condition; the velocity components and the water surface elevations at the inlet and outlet of the wave flume are imposed by the RZ method.
For a grid mesh convergence study, 4 different grid mesh sizes *dh* are tested. The grid cells have a resolution of Δ*x* in the horizontal direction and Δz in the vertical direction as shown in table 1. Additionally, the mesh is refined around the free surface leading to a cell aspect ratio of Δx/Δz=5. The time discretization is adjustable and limited by a maximum Courant number condition of *maxCo*=0.4 in the whole computational domain. Figure 1 depicts the free surface elevation (η) profiles as a function of the numerical wave tank length at the time of 15 times of the wave period. It is shown that the numerical elevation conforms to the required value (theory) for the four grid mesh sizes.

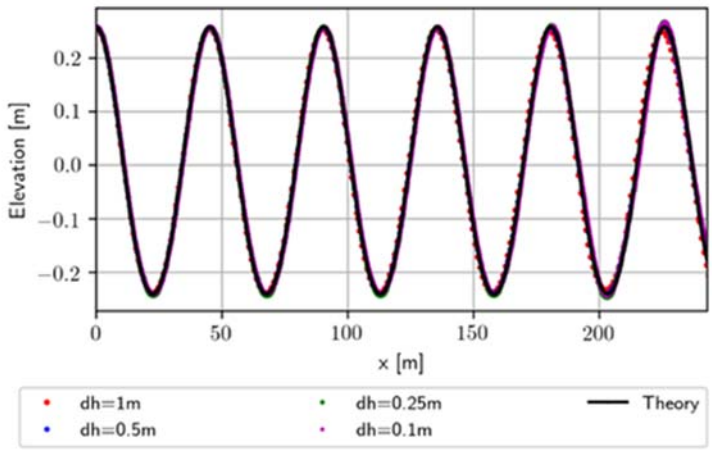

Figure 1. Mesh convergence study for wave propagation.

A thorough validation with theory is made by means of the Root Mean Square Error (RMSE) which reads:

$$RMSE = \sqrt{\frac{1}{N}\sum_{i=1}^{N}(\eta_{Ti} - \eta_{Ni})^2}, \quad (11)$$

where η_T are the theoretical values and η_N are the corresponding numerical data. Indeed, the lower the RMSE, the better a given mesh is able to fit to the theoretical data.
The results provided by the calculation of RMSE are listed in table 1. The average RMSE values over the validation dataset are very low, it means that the numerical model is able

to accurately reproduce the Stokes second order wave theory. Moreover, the RMSE value of dh_4 reveals that this numerical model achieves its best accuracy with this discretisation.

Table 1. Mesh parameters and the RMSE values.

Mesh size dh	***λ/Δx***	***H/Δz (Refinement region)***	***Total number of cells***	***RMSE***
dh_1 = 1 m	*45*	*2*	*3816*	*0.08*
dh_2 = 0.5 m	*90*	*5*	*15264*	*0.07*
dh_3 = 0.25 m	*180*	*10*	*61056*	*0.06*
dh_4 = 0.1 m	*450*	*25*	*381510*	*0.06*

According to these results, the validated numerical model is used to reproduce the experiments performed by RAVINDAR *et al*., (2020) and RAVINDAR & SRIRAM (2021) for a Stokes second order waves of 0.7m height and 6s period at a water depth of 4.1m (see figure 2).

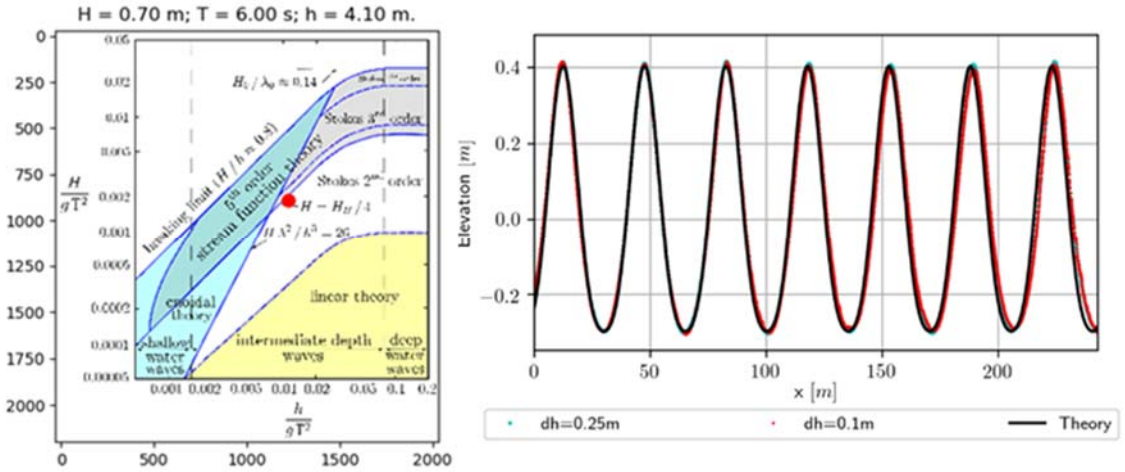

Figure 2. (left) RAVINDAR et al.,(2020) proposed wave theory (LE MÉHAUTÉ, 1976) and (right) Grid mesh convergence study for the same wave theory.

The two finest discretizations dh_3 and dh_4 were used to validate the wave propagation of this model following the same solving procedure as above. The results are shown in figure 2. Although our numerical model generates the desired waves, the discrepancies are a little more highlighted in this case; the wave theory used here is actually very close to the Stokes third order theory as shown in LE MÉHAUTÉ (1976), see figure 2, and this distorts somehow the actual second order waves.

As previously, a RMSE was evaluated to compare the theoretical and numerical data. The RSME value is 0.09 for both dh_3 and dh_4. The discretization dh_4 is finally chosen for the next simulations.

3.2 Waves impact onto a vertical wall

3.2.1 Numerical setup

A 2D numerical setup to model the wave breaking impact is presented in this section. For these first computations, the recurved parapet is not considered but the remaining geometry is maintained as in the experiments of RAVINDAR *et al*., (2020) and RAVINDAR &SRIRAM (2021), see figure 3.

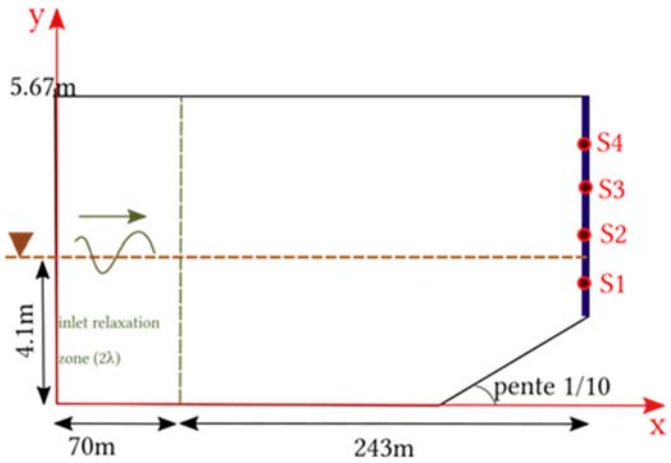

Figure 3. Numerical wave tank sketch.

The experiments were performed in a 307 m long, 5 m width and 7 m height wave flume equipped with a piston type wavemaker to generate waves. The vertical wall is located at a distance of 243 m from the wavemaker, at the end of a 1/10 sloping beach. More details are given in RAVINDAR *et al*., (2020) and RAVINDAR & SRIRAM (2021).
Numerically, the waves are generated using the RZs technique; a cell size of 0.1m is used for meshing the geometry with a refinement around the free surface, the sloping beach and the vertical wall. Multiple pressure probes were added on the vertical wall and several wave gauges were positioned along the numerical tank for analysing the impact pressure and validating our numerical approach.
A simulation of 1080s is performed as in the experiments, with a maximum Courant number of 0.4 using both compressible and incompressible solvers. The laminar flow model is selected for all the computations. It took 12h with 140 cores in CRIANN (Centre Régional d'Informatique et d'Applications Numériques de Normandie).

3.2.2 Free surface elevation

Two wave gauges WG1 and WG2, positioned 50m and 235m respectively from the wave generating zone are added to our numerical tank. We recall that the wave generation in the numerical simulation is via the relaxation zone which is different from wave generation by piston wavemaker in the experiments, therefore, the WG1 was used to

validate the incident waves in the numerical tank. Both numerical (compressible) and experimental time histories of the free surface elevation at WG1 and WG2 are shown in figure 4, and a zoom within the first 500s was made to better visualize the trends.

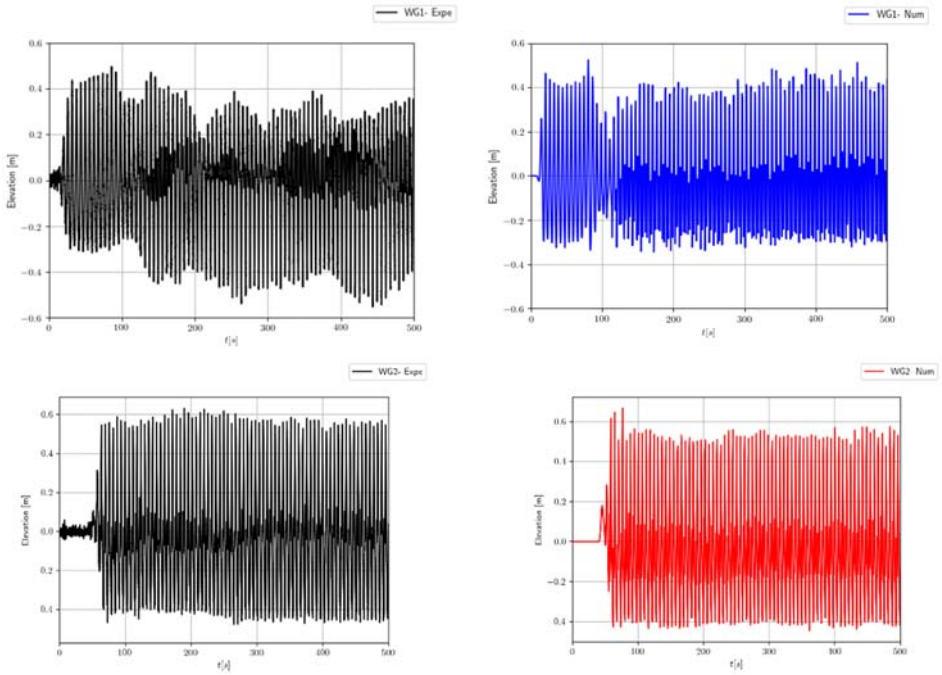

Figure 4. Time series of the free surface: (top left) WG1 experiments, (top right) WG1 present numerical, (bottom left) WG2 experiments, (bottom left) WG2 present numerical.

It can be seen from the results of WG2 placed close to the vertical wall, that the present numerical model has accurately represented the free surface elevation and correctly captured the waves crest values with a very slight difference, the maximum elevation values obtained by the numerical model and the experiments are 0.666m and 0.631m respectively and the minimum ones are respectively -0.446 and -0.514m. So far WG1 is concerned, we notice that actually the way the waves are generated impacts slightly the free surface pattern. However, when comparing the maxima (0.561m and 0.496m) and minima (-0.361 and -0.561) of the present numerical and the experiments respectively, we agree that the incoming waves in the numerical tank are close to the experiments.

3.2.3 Pressure impact on the vertical wall

Both numerical compressible and incompressible results, as well as the corresponding experimental data (black graph) for the pressure impact distributions along the vertical wall are shown in figure 5 where a zoom on the first 300s was made to allow a close-up view of the pressure profiles. It can be seen on the overall sample, that the present

numerical models have correctly captured all the main physical features of the breaking wave interaction with the vertical wall. The plotted profiles are very close to those captured by RAVINDAR & SRIRAM (2021) in their experiments. It can also be seen that the numerical plots are noiseless and some obvious shift and differences are noticeable. To better assess the differences a statistical analysis should be done.

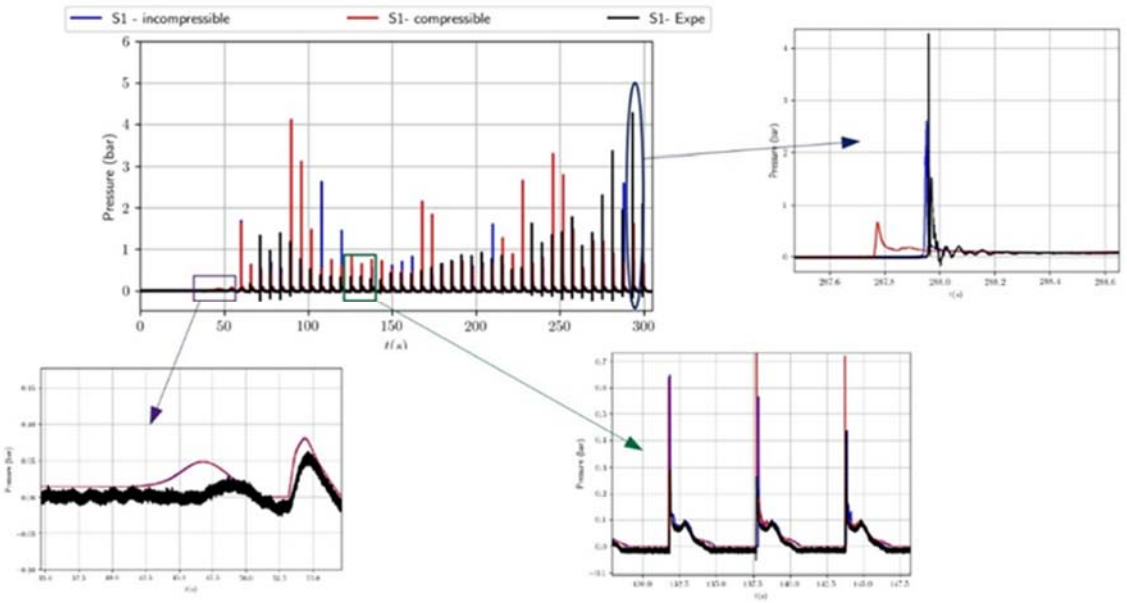

Figure 5. Impact pressure on the wall recorded by the pressure sensor S_1 at the impact location h=3.96m.

4. Conclusion

Compressible and incompressible solvers within the OpenFOAM package have been used in the present work to simulate the breaking wave impact on a vertical wall. The relaxation zone method of the waves2Foam toolbox has been succeffully applied to validate the wave generation and absorbing capacities of the numerical model.

Comparisons between the present numerical results and the experimental data for free surface elevation and the pressure impact have shown that OpenFOAM can accurately model the Stokes second order wave impact on an offshore structure. The present study being still in progress, we aim at presenting during the conference, simulations of breaking waves impact on a vertical structure with a recurved parapet with a more comprehensive loading assessment.

5. References

BATLLE MARTIN M. (2021). *Computation of extreme wave impact on wave energy converters attached to coastal protection structures*. PhD thesis, University of le Havre Normandie. https://tel.archives-ouvertes.fr/tel-03355413b

COOKER M.J., PEREGRINE D.H. (1992). *Wave impact pressure and its effect upon bodies lying on the sea bed.* Coastal Engineering. Volume 18, issues 3-4, pp. 205-229. https://doi.org/10.1016/0378-3839(92)90020-U

COURANT R., FRIEDRICHS K., LEWY H. (1967). *On the partial difference equations of mathematical physics*. IBM J. Res.Dev. Vol 11- Issue 2, pp 215–234.

DE ROUVILLE A., BESSON P., PETRY P. (1938). *Etat actuel des études internationales sur les efforts dus aux lames.* Ann. Ponts Chaussées, vol.108, pp.5-113.

FERZIGER J.H., PERIC M. (1999). *Computational methods for fluid dynamics*, second ed. Springer, Berlin, 440 p.

FUHRMAN D.R., MADSEN P.A, BINGHAM H.B. (2006). *Numerical simulation of lowest-order short-crested wave instabilities.* Journal of Fluid Mechanics, 563:415-441.

HIRT C.W., NICHOLS B.D. (1981). *Volume of fluid (VOF) method for the dynamics of free boundaries*. Journal of Computational Physics. Vol 39, pp 201–225. https://doi.org/10.1016/0021-9991(81)90145-5

ISSA R.I. (1986). *Solution of the implicitly discretised fluid flow equations by operator splitting*. J. Comput. Phys. 62, 40–65. https://doi.org/10.1016/0021-9991(86)90099-9

JACOBSEN N.G., FUHRMAN D.R., FREDSOE J. (2012). *A wave generation toolbox for the open-source CFD library: OpenFOAM.* International Journal of Numerical Methods in Fluids, Vol 70-Issue 9, pp 1073-1088.

LE MEHAUTE B. (1976). *An introduction to hydrodynamics and water waves.* Springer study Edition. Springer, Berlin, Heidelberg. https://doi.org/10.1007/978-3-642-85567-2_18

LIU S., GATIN I., OBHRAI C., ONG M.C., JASAK H. (2019). *CFD simulations of violent breaking wave impacts on a vertical wall using a two-phase compressible solver*. Coastal Engineering. Vol 154, 103564.

MORGAN G.C.J., ZANG J., GREAVES D., HEATH A., WHITLOW C., YOUNG J. (2010). *Using the rasinterFoam CFD model for wave transformation and coastal modelling.* Coastal Engineering, n°32, https://doi.org/10.9753/icce.v32.waves.23

OUMERACI H., KLAMMER P., PARTENSCKY H.W. (1993). *Classification of breaking wave loads on vertical structures*. Journal of Waterway, Port, Coastal and, Ocean Engineering. Vol 119, no 4, pp 381–397. https://doi.org/10.1061/(ASCE)0733-950X(1993)119:4(381)

RAVINDAR R., SRIRAM V., SCHIMMELS S., STAGONAS D. (2019). *Characterization of breaking wave impact on vertical wall with recurve.* ISH Journal of Hydraulic Engineering, Vol.25, (2), pp 153-161, https://doi.org/10.1080/09715010.2017.1391132

RAVINDAR R., SRIRAM V., SCHIMMELS S., STAGONAS D. (2020). *Large scale and small-scale effects in wave breaking interaction on vertical wall attached with large recurve parapet.* Coastal Engineering, Volume 36v, papers.22. https://doi.org/10.9753/icce.v36v.papers.22

RAVINDAR R., SRIRAM V. (2021). *Impact pressure and forces on a vertical wall with different types of parapets.* Journal of Waterway, Port, Coastal and Ocean Engineering, Vol. 147, Issue 3. https://doi.org/10.1061/(ASCE)WW.1943-5460.0000635